

# HiSST: 4th International Conference on High-Speed Vehicle Science Technology

22 -26 September 2025, Tours, France



## Development of UHTC Materials and high Temperature Characterizations using CO<sub>2</sub> Laser Beam

<u>Aurélie Julian-Jankowiak</u><sup>1</sup>, Jean-François Justin<sup>2</sup>, Antoine Débarre<sup>3</sup>, Damien Bautista<sup>4</sup>

#### **Abstract**

Ultra-High Temperature Ceramics (UHTC) are good candidates to fulfil the harsh requirements of hypersonic applications such as very high temperatures (>2000°C) and oxidizing atmospheres. In this context, Onera is working on the development of new UHTC compositions and UHTC matrix composites (UHTCMC) but also on the development of home-made laser test benches (3 kW CO<sub>2</sub>) allowing the coupling or decoupling of thermal, mechanical et chemical stresses. Thus, the influence of the composition on the oxidation mechanisms of UHTC were studied in several oxidizing conditions through post-mortem scanning electron microscope examinations or using real-time monitoring of thermal oxidation. This work is focused on monolithic materials with optimised composition based on diborides compounds and composites with different ultrarefractory matrices. After manufacturing and microstructural characterizations (particle size, porosity and composition, UHTC and UHTCMC samples were submitted to high thermal flux under air or water vapour. Then, ultra-high temperature laser thermogravimetric analysis is used to track the sample weight during oxidation in air. The main interest is to study the mass variation above 1600°C in air and with very high heating rate. These characterizations allow us to propose more precise oxidation mechanisms with temperature. Afterwards, samples are characterized with SEM/EDS to confirm the oxidation mechanisms. For example, at 2000°C, weight gain is lower for ZrB<sub>2</sub>-based materials than for HfB2-based ones. However, final microstructures are strongly different and the SiC-depleted layer is 7-times larger for HfB2-based materials.

Keywords: UHTC; UHTCMC; Laser; SPS; High thermal flux

#### **Nomenclature**

BLOX4	Banc Laser d'Oxydation n°4 (4 <sup>th</sup> laser	TGA	ThermoGravimetric Analysis
	oxidation analysis facility)	UHTC	Ultra-High Temperature Ceramics
CMC	Ceramic Matrix Composite	UHTCMC	Ultra-High Temperature Ceramic
CTE	Coefficient of Thermal Expansion		Matrix Composites
EDM	Electrical Discharge Machining	XRD	X-Ray Diffraction
EDS	Energy Dispersive Spectroscopy	ρ	Density (in g/cm3)
PIP	Polymer Infiltration and Pyrolysis	$\sigma_{f}$	Bending flexural strength (in MPa)
PyC	Pyrolytic Carbon	<b>ε</b> f	flexural strain (in %)
RMI	Reactive Melt Infiltration	<b>d</b> 50	Median particle size (in µm)
SEM	Scanning Electron Microscope	E	Young's modulus (in GPa)
SiC	Silicon Carbide	$E_f$	Flexural modulus (in GPa)
SIP	Slurry Infiltration Process	$K_{1C}$	Fracture toughness (in MPa.m <sup>1/2</sup> )
SPS	Spark Plasma Sintering	Hv	Hardness (in GPa)

<sup>&</sup>lt;sup>1</sup> DMAS, ONERA, Université Paris-Saclay, 92320 Châtillon — France, aurelie.jankowiak@onera.fr

HiSST-2025-281 Page | 1
Development of UHTC Materials and high Temperature Characterizations using CO<sub>2</sub> Laser Beam Copyright © 2025 by author(s)

<sup>&</sup>lt;sup>2</sup> DMAS, ONERA, Université Paris-Saclay, 92320 Châtillon – France, jean-francois.justin@onera.fr

<sup>&</sup>lt;sup>3</sup> DMAS, ONERA, Université Paris-Saclay, 92320 Châtillon – France, antoine.debarre@onera.fr

<sup>&</sup>lt;sup>4</sup> DMAS, ONERA, Université Paris-Saclay, 91120 Palaiseau – France, damien.bautista@onera.fr



#### **HiSST: 4th International Conference on High-Speed Vehicle Science Technology** 22 -26 September 2025, Tours, France



#### 1. Introduction

Since the 2000s, the pursuit of hypersonic flight vehicles has rekindled interest in Ultra High Temperature Ceramics (UHTC) materials. Specifically, hypersonic vehicles with sharp aerodynamic surfaces (engine inlets, wing leading edges, and nose caps) require materials that can withstand temperatures between 2000°C to 2400°C in oxidizing environments and even, being reusable. These conditions exceed the operational limits of current high-temperature structural materials, such as SiC or Si<sub>3</sub>N<sub>4</sub>-based materials, which only exhibit good oxidation resistance up to approximately 1600°C. C/C composites can be used at higher temperatures but for very short time in oxidizing atmosphere at such temperatures. Thus, the development of high temperature structural materials for oxidizing and rapid heating environments is of paramount engineering importance. Several investigations have highlighted the suitability of UHTCs for meeting these stringent requirements [1-5].

UHTCs, comprising borides, carbides, and nitrides (e.g., ZrB2, HfB2, ZrC, HfC, TaC, HfN), are characterized by high melting points, exceptional hardness, chemical inertness and relatively good oxidation resistance in severe environments. Furthermore, UHTC materials possess high thermal conductivity, which provides excellent thermal shock resistance and makes them ideal for numerous high-temperature applications. For instance, on a leading edge, high thermal conductivity reduces thermal stresses within the material by minimizing the internal temperature gradient. This also enables efficient heat dissipation from the component's surface. Moreover, diboride-based UHTCs exhibit high electrical conductivity, facilitating the manufacture of complex shapes via Electrical Discharge Machining (EDM).

In recent years, ONERA's Materials and Structures Department has been engaged in various projects focused on UHTC material development, from manufacturing to thermomechanical assessments and oxidation resistance understanding [6-15]. Our primary research efforts have concentrated on monolithic zirconium and hafnium diborides (ZrB2 and HfB2), which exhibit extremely high melting points (>3200°C), excellent thermomechanical properties and enhanced oxidation resistance with the addition of ~20%vol. SiC [5,16]. Compared to carbides and nitrides, diborides also display higher thermal and electrical conductivities, ensuring good thermal shock resistance and machinability (via EDM). However, the use of monolithic ceramics for high-temperature structural applications is limited by drawbacks such as low fracture toughness. This has led to increased interest in UHTC matrix composites (UHTCMCs) [17-23] and most of the present papers deal with these composite materials. Several processing routes are studied in the literature as Reactive Melt Infiltration (RMI) [18, 21], Slurry Impregnation (SIP and sintering [20], Polymer Infiltration and Pyrolysis (PIP), ... Most of these works consider UHTC matrix reinforced with a continuous fibre fabric. Consequently, our recent activities have shifted focus towards continuous fibre-reinforced composites, with a preference for boride-based compositions.

This paper presents a synthesis of our research findings on UHTC materials from monoliths to composites based on model materials and also the development of new test benches. Several aspects are exposed and notably their manufacturing, their properties and their oxidation resistance.

#### 2. Materials manufacturing

#### 2.1. Monolithic ceramics

ZrB<sub>2</sub>-SiC and HfB<sub>2</sub>-SiC compositions with or without additives have been selected as model materials for our studies. Y2O3 additive was used to make the sintering process easier but also to enhance oxidation resistance at high temperature. Commercially available ZrB2, HfB2, SiC and Y2O3 powders were employed to manufacture the materials and their properties are listed in Table 1.

**Table 1.** Grade, purity, particle size and measured density of starting powders

Powder	Grade / Supplier	Purity (%)	Particle size d₅₀ (μm)	Density
ZrB <sub>2</sub>	Grade B / H.C Starck	>97.8	2.8	5.98
HfB <sub>2</sub>	Grade A / H.C Starck	>97.0	7.6	10.66
SiC	BF12 / H.C. Starck	>98.5	0.6	3.15
Y <sub>2</sub> O <sub>3</sub>	Ampere Industrie	99.99	<5.0	4.89

To obtain the selected compositions, starting powders were weighed according to their respective proportions and attrition milled in ethanol using  $ZrO_2$  or WC media. Then, the mixtures were dried in a rotary evaporator and sieved down to 50  $\mu$ m mesh size to avoid agglomeration. Finally, the powder blends were sintered in coated graphite dies (Papyex®) by Spark Plasma Sintering (SPS). Compositions and sintering parameters are reported in Table 2.

**Table 2.** Sintering parameters of several monolithic samples

Method	Sample size	Composition	Reference	Sintering parameters
SPS	Ø40 mm discs	ZrB <sub>2</sub> /20vol% SiC ZrB <sub>2</sub> /20vol% SiC/3vol% Y <sub>2</sub> O <sub>3</sub> HfB <sub>2</sub> /20vol% SiC HfB <sub>2</sub> /20vol% SiC/3vol% Y <sub>2</sub> O <sub>3</sub>	ZS ZSY HS HSY	1850°C/15min/30MPa/Argon 1850°C/15min/30MPa/Argon 1850°C/15min/30MPa/Argon 1850°C/5min/30MPa/Argon

#### 2.2. UHTC Composites

For UHTCMC, materials based on borides matrix reinforced with continuous carbon fibres have been preferentially investigated ( $C_f$  /  $HfB_2$ - 20 vol% SiC in particular). The selected process to obtain these composites was a hybrid process coupling fibre impregnation with a slurry and Polymer Infiltration and Pyrolysis (PIP) [22-23]. This process allows a better control of the final composition compared to one step infiltration process (powder + precursor in the same slurry) [13]. The selected raw materials for these composites were a 2D carbon fibre fabric (Toho Tenax HTA5131, 3K, twill weave 2x2, 282 g/m²) for the reinforcement and a combination of  $HfB_2$  powder (Table 1) and a SiC precursor (Starfire Systems SMP-10) for the matrix.

First, PyC interphase is deposited on the C<sub>f</sub> fabrics using a CVD technique. The thickness of the interphase is around 250nm but some tests were performed increasing this thickness.

In parallel,  $HfB_2$  powders are attrition milled in ethanol using WC media as for monolithic ceramics to reduce the particle size (<1µm) and favour a good infiltration of the powder in the fabric. Then, a  $HfB_2$  water-based slurry is prepared using PEI as dispersant agent. The C fabrics are impregnated with the  $HfB_2$  slurry, dried and weighed to reach the targeted amount of  $HfB_2$ . After this impregnation step, a sintering step at 1650°C is performed to set the final volume of the composite and the fibre volume fraction. After this step, the open porosity in the composite is around 20%. The composite is then placed in a specific mould ( $40 \times 50 \text{ mm}^2$ ) for the PIP step. The infiltration is realised by applying vacuum on one side of the mould in order to suck the SiC precursor located in a recipient connected to the other side of the assembly.

After infiltration, samples are dried and hot pressed in graphite die (at 1600°C/50 MPa/1h) under flowing argon to fully transform the precursor in crystalline SiC. This PIP step is repeated several times (at least 6 times) until open porosity is less than 10%.

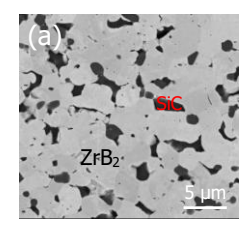
#### 3. Materials characterisation

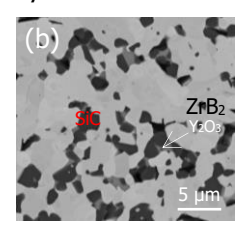
Concerning the UHTC monoliths notably, a thorough characterisation of their properties has been achieved in several studies [7, 12, 13]. Several aspects have been studied: microstructure (X-Ray diffraction), chemical, physical, mechanical, thermal and optical properties (diffusivity, heat capacity,

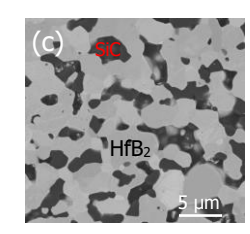
CTE, emissivity), machining behaviour, oxidation resistance in severe environment and so on. The bulk density and open porosity of materials were measured by the Archimedes' method. The level of densification was calculated as the ratio of the apparent density on the theoretical density. Microstructures were observed on polished cross-sections using a Scanning Electron Microscope (SEM) equipped with energy dispersive spectroscopy (EDS) for local analysis. Bending flexural strength has been determined by four points flexural tests. Young's moduli were measured by impulse excitation of vibration on bars ( $\sim$ 35.1 x 5.2 x 2.1 mm³) using a Grindosonic MK5 apparatus [24]. Hardness (Hv) and fracture toughness ( $K_{IC}$ ) were obtained on ¼ µm polished surfaces by Vickers' indentation with a load of 98 N. The fracture toughness ( $K_{IC}$ ) is estimated by crack length measurement of the radial crack pattern formed around Vickers indents [25]. Thermal expansion coefficients were determined up to 1440°C with a heating rate of 5°C/min under flowing argon (20 ml/min) using a SETSYS Evolution SETARAM dilatometer. The oxidation behaviour was studied from 1200°C to 2400°C with a specific test bench using a 3 kW  $CO_2$  laser under air and water vapour atmospheres. Moreover, high temperature thermogravimetric test bench has been developed to follow mass variation at very high temperature under air atmosphere.

### 3.1. Monolithic ceramics properties 3.1.1. Microstructure

Densification levels measured on all types of monoliths are superior to 96% of the theoretical density and open porosities lower than 1%. Microstructural aspects of these materials after SPS are presented in Fig. 1. We can see than very fine microstructures are obtained with a good homogeneity and small grain sizes. SiC is finely and randomly distributed in the  $ZrB_2$  or  $HfB_2$  matrices. In the case of  $Y_2O_3$ -containing materials areas rich in  $Y_2O_3$  are detected using EDS and correspond to cubic phases of  $ZrO_2$ - $Y_2O_3$  or  $HfO_2$ - $Y_2O_3$  from XRD analyses.







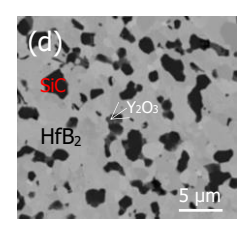


**Fig. 1.** SEM micrographs of (a)  $ZrB_2/20$  vol.%. SiC, (b)  $ZrB_2/20$  vol.%. SiC/3 vol.%  $Y_2O_3$ , (c)  $HfB_2/20$  vol.%. SiC and (d)  $HfB_2/20$  vol.%. SiC/3 vol.%  $Y_2O_3$  monoliths densified by SPS

#### 3.1.2. Mechanical behaviour

Mechanical properties, at room temperature, of several monolithic samples are reported in Table 3. The mechanical behaviour of these monoliths is very interesting with flexural strength values up to 850MPa and high Young's moduli (400-500GPa). Moreover, it is important to notice than at high temperature some of these properties are sometimes even higher (flexural strength in particular) [7].

**Table 3.** Density, Young's Modulus, bending flexural strength, fracture toughness, hardness and coefficient of thermal expansion of materials sintered by SPS

Monolith reference	ρ <b>(g/cm³)</b>	E (GPa)	o <sub>f</sub> (MPa)	K <sub>1C</sub> (MPa.m <sup>1/2</sup> )	H <sub>v</sub> (GPa)	CTE (.10 <sup>-6</sup> °C <sup>-1</sup> )
ZS	5,32		468 ± 147*	3,5 ± 0,7	15,3 ± 0,6	7,8 (25-1440°C)
ZS	5,65	$416 \pm 3$	$584 \pm 82$			7,7 (25-1440°C)
HS	9,19	$479 \pm 11$	$694 \pm 91$	$6,7 \pm 0,9$	$17,5 \pm 0,3$	7,4 (25-1440°C)
HSY	9,04	$489 \pm \ 4$	$843\pm110$	$3,9 \pm 0,3$	$\textbf{21,9} \pm \textbf{1,1}$	<b>7,5</b> (25-1440°C)

<sup>\*</sup>bi-axial flexural strength

In a previous study, these monoliths have been used to manufacture prototypes and realistic components which have been tested in a combustion test bench [8, 9, 13].

#### **3.1.3.** Oxidation resistance

Several test campaigns have been carried out in order to investigate the thermal and chemical resistance of the monoliths. Most of them were performed with a home-made device (BLOX4). BLOX4

is a facility used for oxidation tests at very high temperatures (up to 2500°C) in controlled atmospheres ( $H_2O$ , Ar,  $N_2$ ,  $H_2$ , air ...) at pressures ranging from few millibars to 4 bar. Heating of discs samples is ensured thanks to a  $CO_2$  laser (3 kW). Surface temperature of the monoliths is measured with two bicolor pyrometers. A schematic view of this device as well as a  $\emptyset$  20 mm disc sample ( $HfB_2$ / 20vol% SiC/ 3vol%  $Y_2O_3$ ) before and during a test at 1800°C is presented in Fig. 2.

In the framework of a PhD ZS, HS and HSY densified by SPS have been specifically studied at very high temperature under oxidative atmosphere [11, 12, 14, 15]. All experiments were conducted at a constant total pressure of 1 bar within a controlled atmosphere comprising 30% water vapor (H2O) and 70% argon (Ar) in volume. The testing protocol involved initially ramping up the laser power to reach 1000°C, followed by a precisely controlled temperature increase at a rate of 5°/s. This gradual heating enabled the sample to achieve the desired temperature, ranging from 1200°C to 2400°C, where it was held for a predetermined dwell time before being cooled down at the same rate.

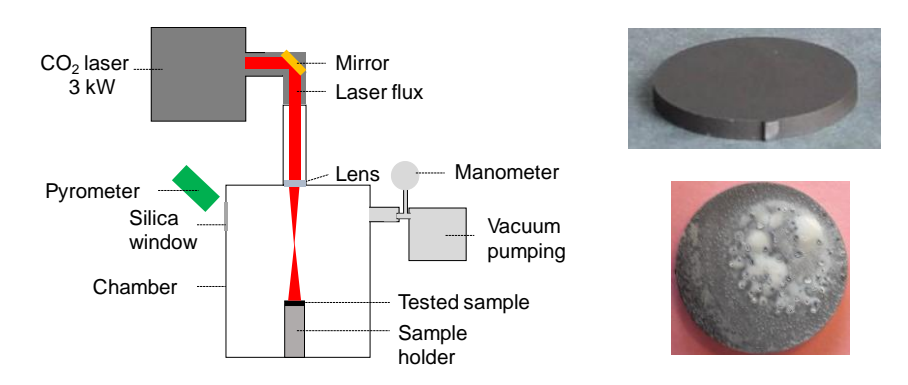


**Fig. 2.** Schematic representation of the BLOX4 device, disc sample after machining and surface of a ZS material after a test at 1600°C

After the tests, cross-sections of the samples are observed through SEM examinations to study the oxidation mechanisms (Fig. 3).

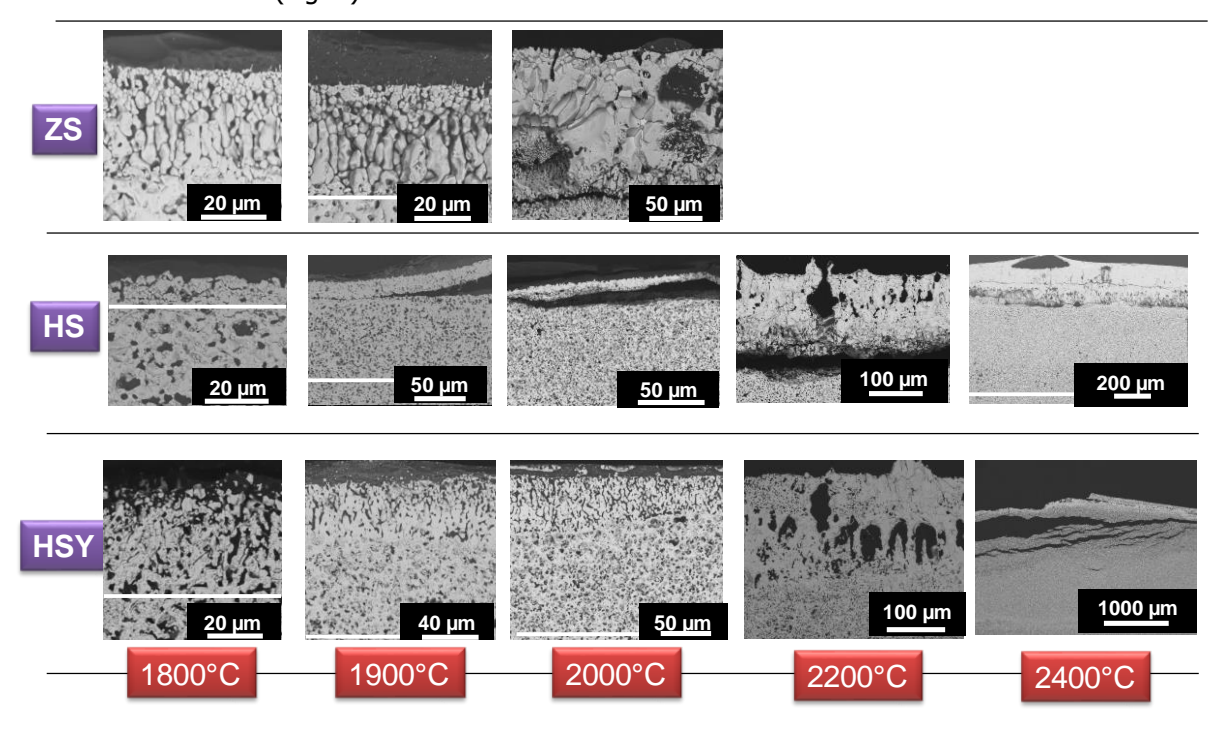


**Fig. 3.** SEM examinations of cross-section of ZS, HS and HSY samples after tests at 1800, 1900, 2000, 2200 and 2400 $^{\circ}$ C in the BLOX4 facility (30%H<sub>2</sub>O/Ar)

Below 1500°C, very thin oxidised layers are formed. From 1550°C, ZS, HS and HSY exhibit a two-layered oxide scale made of a glassy SiO<sub>2</sub> rich layer on the top and beneath an HfO<sub>2</sub> or ZrO<sub>2</sub> layer. At 1900°C, a three-layered oxide scale is observed for all the compositions: a heterogeneously distributed glassy silica rich layer on the top, an HfO<sub>2</sub> or ZrO<sub>2</sub> layer and then a SiC-depleted HfB<sub>2</sub> or ZrB<sub>2</sub> layer. Moreover, some mechanical damages (non-cohesive lamellae) are observed on materials that do not contain  $Y_2O_3$ . At 2000°C, some mechanical issues are detected for ZS samples and a non-adherent oxide layer is present on HS. However, for HSY, oxide layers are still adherent even if the top HfO<sub>2</sub> layer contains cracks. This good behaviour is due firstly to the monoclinic to tetragonal transition of HfO<sub>2</sub> which is less preponderant in HSY than in HS and secondly to the creation of an  $Y_2Si_2O_7$  interphase (between HfO<sub>2</sub> and the SiC-depleted HfB<sub>2</sub> layer) that mitigates the thermal mismatch. The same observations are made at 2200°C. At 2400°C, despite some mechanical damages, the HfO<sub>2</sub> top layer at the surface of HS samples exhibits evidence of sintering and might provide further resistance towards oxidation. At this temperature, HSY samples exhibit detrimental mechanical issues with strong delamination and spallation.

Then to have a better understanding of weight variation during high temperature test in oxidative atmosphere a new "high temperature thermogravimetric analysis" test bench has been developed, also named Laser TGA. A schematic view is proposed in Fig. 4Fig. 4. As for the BLOX4 facility, the same CO<sub>2</sub> laser is used to heat the surface of the sample. Surface temperature of the monoliths is measured with one bicolor pyrometer and an IR camera. An optical camera is used to follow the sample during the test. Weight variations of the samples are measured using a scale with a precision of 0.01mg. The tests are performed in air laboratory without any flow.

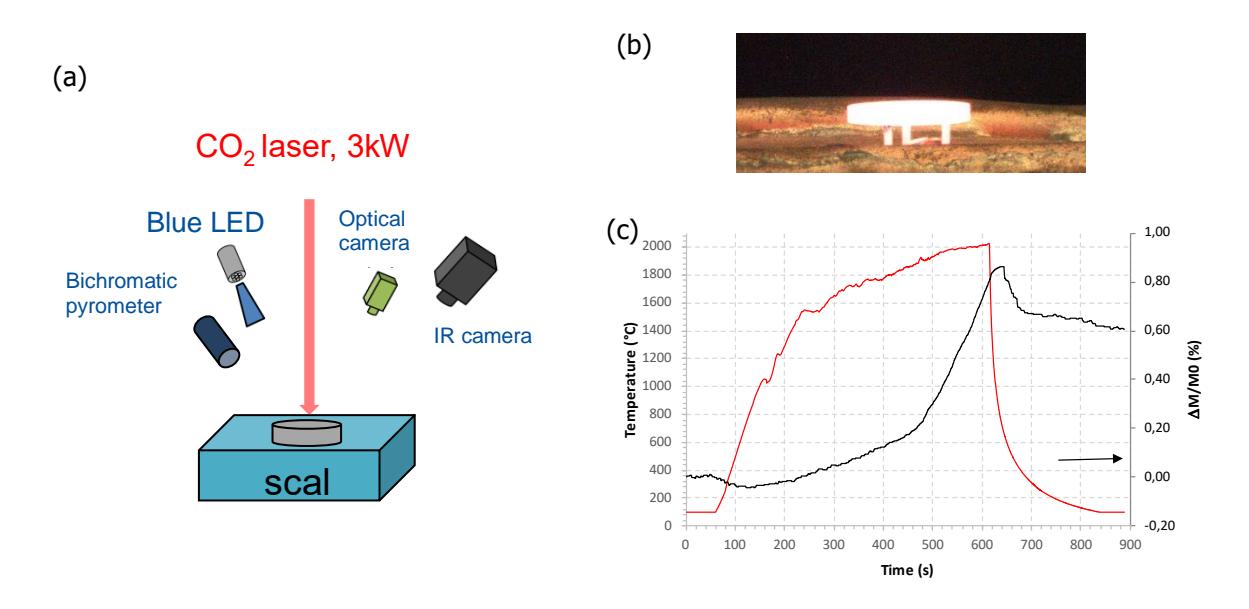


**Fig. 4.** (a) schematic view of the high temperature thermogravimetric analysis in oxidative atmosphere test bench, b) a sample during the test and (c) example of weight variation during a heating ramp

From Fig. 4, it can be seen that the heating rate is slow down when weight gain begins to increase. Moreover, weight gain is always measured whereas strong evaporation is observed through the cameras. Comparison of the weight gains of three different compositions is presented in Fig. 5 a. Cross-sections of ZSY and HS after the test at  $2000^{\circ}$ C are presented in Fig. 5 c and d. Both materials exhibit glassy phase at the surface and it is very rich in  $ZrO_2$  in the case of ZS. This is also visible on the photos Fig. 5 as the surface of ZSY is white due to the  $ZrO_2$  phase with some evidence of bubbling, whereas HS seems glassy and quite smooth. The SiC-depleted layer in also detected in both cases and is around  $20\mu m$  for ZSY and  $130\mu m$  for HS. As weight gain is lower for HS than for ZSY, it can be due to SiC evaporation. Thus, the oxidation mechanisms are completely different between the both materials. Finally, HS exhibits a better oxidation resistance but the low weight gain is due to SiC oxidation and evaporation in the underlying layers and its re-condensation at the surface of sample renewing the glassy phase at the surface. In the case of ZSY, the oxide layers at the surface are thicker

than in the case of HS, with a very thin SiC-depleted layer, thus weight gain is higher but evaporation of the glassy layer is favoured at the surface with a slow renewing. Finally, oxidation resistance of ZSY is lower than for HS.

Even if reducing the weight variations is of great interest to improve oxidation resistance, it is not always sufficient. Indeed, it can be seen that weight gain is higher for HSY than for HS whereas cross-sections examinations after the BLOX4 tests allow us to conclude that HSY exhibit a better oxidation resistance than HS up to 2000°C. This experiment confirms that in the case of HSY, the addition of  $Y_2O_3$  allows to modify the viscosity of the glassy phase and then the solubility of  $Y_2O_3$  in the underneath layers. Then, at the surface when  $Y_2O_3$  evaporates, the addition of  $Y_2O_3$  allows the formation of cubic  $Y_2O_3$  and refractory  $Y_2Si_2O_7$  phase increasing the glassy phase viscosity at the surface and thus, limiting its evaporation. These two phases also allow to reduce mechanical issues, avoiding the tetragonal-monoclinic phase transition of the  $Y_2O_3$  phase during the cooling and limiting the CET mismatch between the oxide layers and the layers underneath. Thus, the addition of  $Y_2O_3$  favours weight gain and limits weight loss.

Comparing the influence of the heating rates (Fig. 5b), it can be seen that weight gain is promoted by slow heating rate as thermodynamic equilibrium is reached whereas for high heating rates, oxidation reactions are delayed. Using laser TGA, heating rate is 100 times higher than using classical TGA.

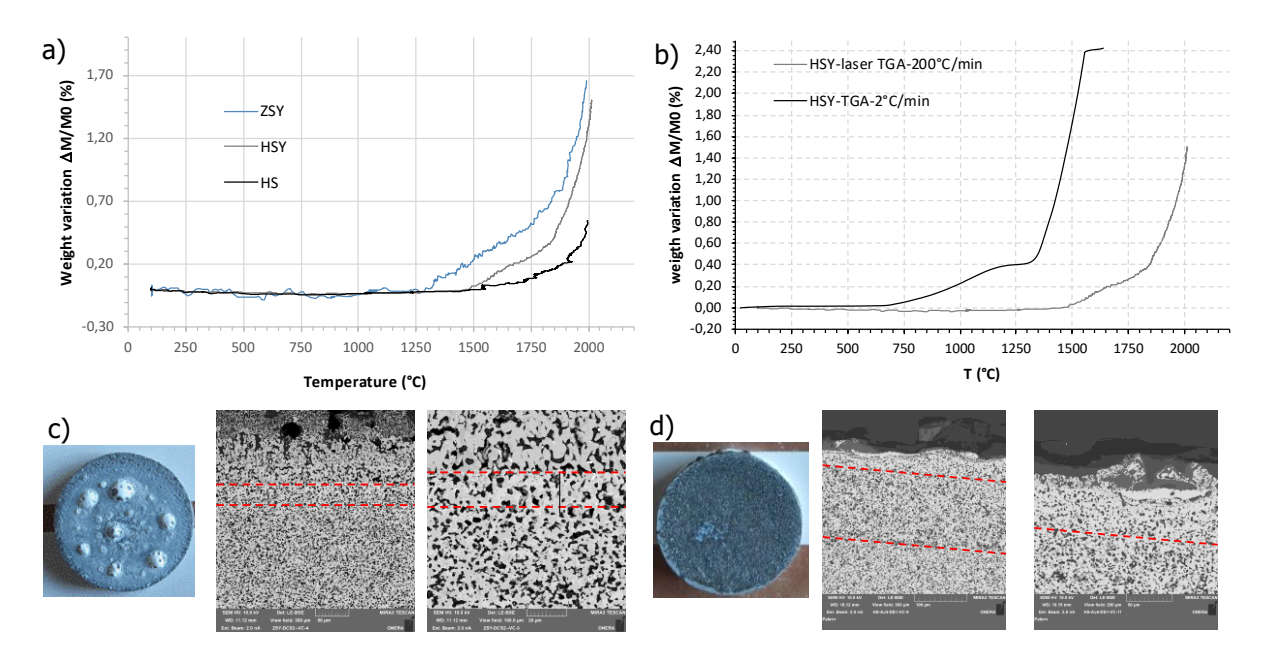


**Fig. 5.** Weight variation for ZSY, HS and HSY samples during a laser TGA test (a), comparison of weight variation between laser TGA and classical TGA tests (b), photography and SEM examination of cross-sections of ZSY after the test at 2000°C (c) and photography and SEM examination of cross-sections of HS after the test at 2000°C (d)

## 3.2. UHTC Composites properties 3.2.1. Microstructure

It is important to notice that for these materials the development phase is still in progress. The PyC matrix/fibre interface is around 250nm in this study (Fig. 6a). The Fig. 6b shows the composite after the slurry impregnation and sintering steps. A particle size gradient is clearly visible in the fabric with the smallest  $HfB_2$  particles in the tow of the fabric. The SiC precursor is sufficiently liquid during the infiltration process to correctly penetrate inside the fibre tows (Fig. 6d).

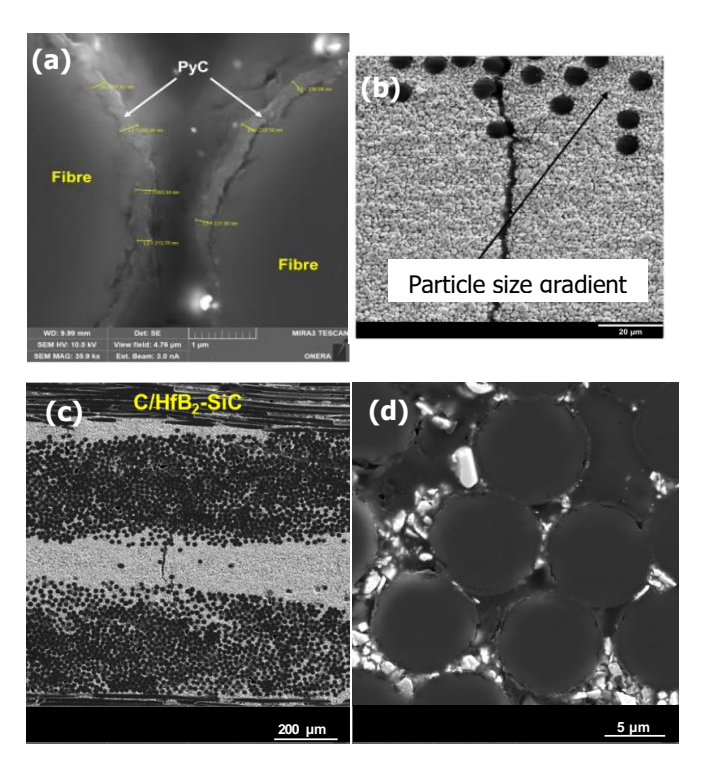


**Fig. 6.** Microstructure of  $C_f/HfB_2$ -SiC composite made by hybrid process coupling fibre impregnation and PIP: (a) the PyC interphase, (b) microstructure after  $HfB_2$  impregnation, (c) and (d) the final microstructure after SiC precursor PIP

Thus, after the final sintering, SiC is randomly distributed between the fibres in a tow whereas  $HfB_2$  is more located around the tows (Fig. 6 c and d). It can be noted that the thermal treatment applied for densification and pyrolysis induces no reaction at the fibre/matrix interface. Moreover, no macro-pores are observed and the porosity is principally composed of small voids and cracks.

#### 3.2.2. Mechanical properties

Several UHTCMCs have been manufactured and the mechanical properties were assessed using 4pts bending tests. This hybrid process and the PyC interphase allows us to greatly improve the mechanical performances of the UHTCMC starting from 70MPa few years ago [13] to 190-250MPa (Fig. 7). Non-brittle failures are observed for all the composites from stress-strain curves and the failure facies (Fig. 7 b and c). Fibre pull out is observed indicating a matrix/fibre decohesion during the mechanical test and thus energy dissipation mechanisms. So, the composite effect is operating.

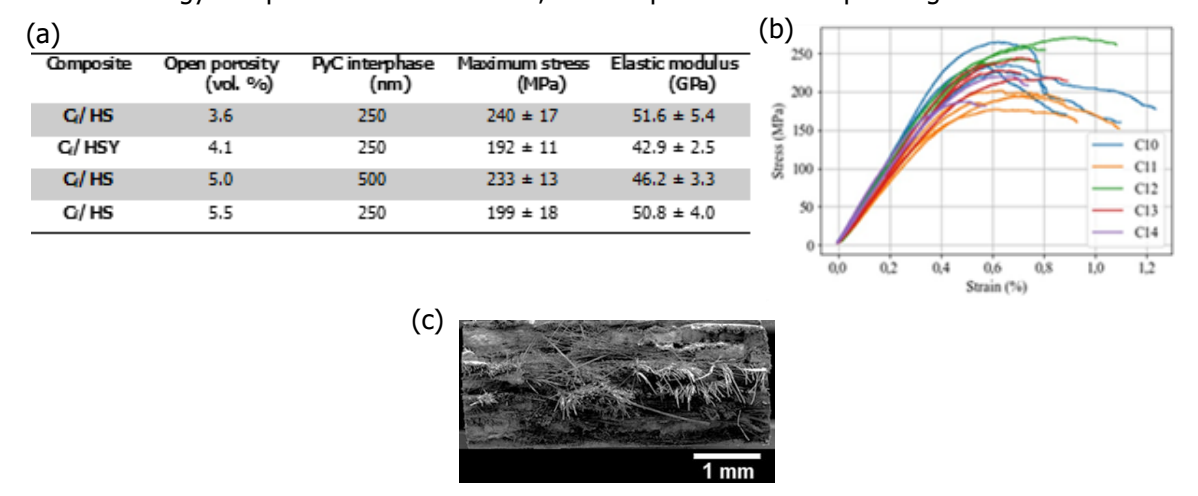


Fig. 7. Mechanical properties of UHTCMCs (a), strain-stress curves (b) and fracture facies (c)

#### 3.2.1. Oxidation resistance

Oxidation resistance of as-processed UHTCMCs is assessed using the previously described BLOX4 (§3.1.3). All experiments were conducted at a constant total pressure of 1 bar within a controlled atmosphere comprising 30% water vapor ( $H_2O$ ) and 70% air. In this case, the heating and cooling rates are imposed to 60°C/s. The following test conditions are studied for  $C_f$ /HS composites: 1600°C-50min; 1800°C-30min and 2000°C-5min.

The morphology of the  $C_f/HS$  after the tests is presented in the Fig. 8. The influence of temperature and time is clearly visible.

1600 °C – 50 min	1800 °C – 30 min	2000 °C – 5 min
45 mm		

Fig. 8. Morphology of the Cf/HS samples after the BLOX4 test under air/30 vol. %H2O

After the tests, the surfaces and the cross-sections of the samples are analysed through SEM and EDS analyses (Fig. 9). First, no delamination is visible on the samples. At  $1600^{\circ}$ C, the centre of the sample is mainly constituted of  $HfO_2$  particles embedded in a  $SiO_2$  glassy phase. At  $1800^{\circ}$ C, the glassy phase is almost no more present at the centre of the sample, only recrystallised  $HfO_2$  is detected. Amorphous  $SiO_2$  is located around the  $HfO_2$ -rich area where the temperature is lower indicating the  $SiO_2$  evaporation in the central zone is due to the temperature and accelerated with the water vapor presence. Then at  $2000^{\circ}$ C, the formation of a dense layer of  $HfO_2$  at the surface of the sample is favoured. This layer contains cracks and pores. Fibres are also visible at surface due to delamination of the oxide layer and the beginning of their degradation in these conditions.

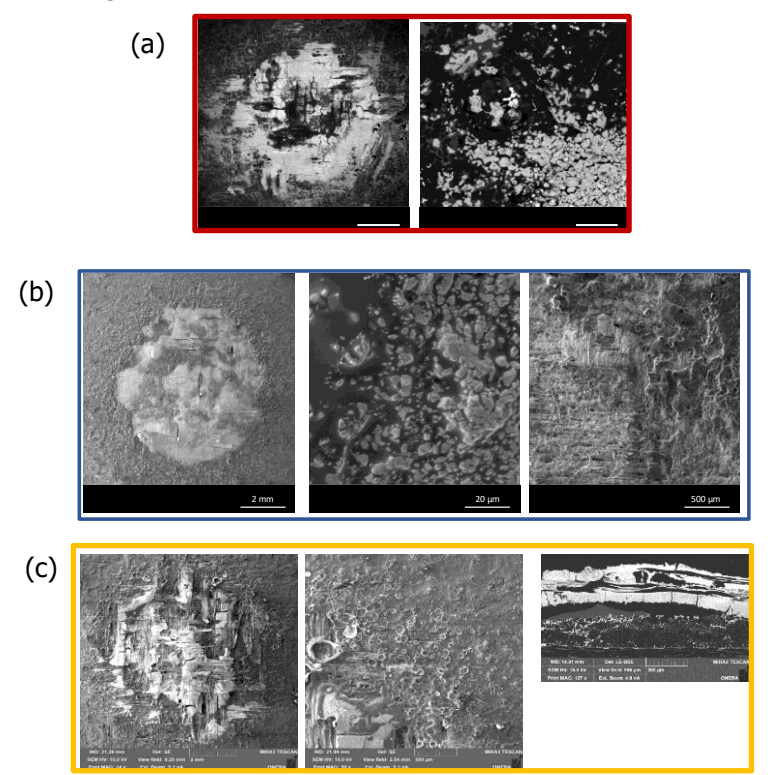


**Fig. 9.** SEM examinations of the surface of the samples Cf/HS after the high temperature tests under air/30vol.%  $H_2O$ : a) at 1600°C-50min, b) at 1800°C-30min and c) 2000°C-5min

Same experiments were performed on C<sub>f</sub>/HSY composites and results similar to ones on monoliths are obtained. HSY favours the formation of a more protective oxide layer at the surface of the composite and limits its spallation.

#### 4. Conclusions and perspectives

Hypersonic and propulsion applications provide some unique thermal-structural challenges (sharp leading edges, air intakes, uncooled injectors, etc.). In order to fulfil the requirements of these components, some specific materials seem to be compulsory: UHTCs. Indeed, thanks to their unique combination of mechanical, thermal and chemical properties, UHTCs are a promising technology for use in a number of high temperature structural applications.

In this context, since more than a decade, Onera is involved in several studies. Most of the work has been focused on monolithic ceramics and now focuses on UHTCMC. For monolithic ceramics, spark plasma sintering (SPS) is the main process to reach high level of densification and avoid grain growth. Thus, screening of the compositions is easy and we have studied mechanical and oxidation resistance properties. For UHTCMC, a hybrid process is used coupling slurry impregnation and precursor polymer infiltration and pyrolysis (PIP). Composites with good powder and precursor distribution are reached without cracks or macropores. For UHTC and UHTCMC, model materials based on ZrB<sub>2</sub>-SiC and HfB<sub>2</sub>-SiC compositions are presented in this paper.

Then mechanical properties are measured using bending tests. Monolithic ceramics exhibit very high mechanical strength (between 500 and 800 MPa) and high Young's moduli (~400-500GPa) but brittle behaviour. This behaviour is reduced with UHTCMCs which exhibit lower mechanical properties (200-250MPa) and young's moduli (~50GPa) but with energy dissipation mechanisms (matrix/fibre decohesion, pull out, ...)

Regarding oxidation resistance, the UHTC and UHTCMC are tested at temperatures higher than 2000°C in oxidative atmospheres using laser test benches. The BLOX4 facility allows to assess the oxidation resistance of the materials under water vapor and the laser thermogravimetric analysis (Laser TGA) allows to monitor weigh variation of the samples under air atmosphere at temperature higher than 1650°C (limit of classical TGA in air). This device was developed in parallel of the material development to improve and complete the characterisation techniques. Lasers permit a very fast heating of the samples giving new information compared to classical furnaces. All these techniques allow to coupled/decoupled the thermal, mechanical and chemical stresses on the samples and enhance our understanding.

Work is now dedicated to the development of UHTCMC materials with new matrices to improve mechanical and oxidation resistance.

#### References

- 1. M.M. OPEKA, I.G. TALMY, J.A. ZAYKOSKI Oxidation-Based Materials Selection for 2000°C + Hypersonic Aerosurfaces: Theoretical Considerations and Historical Experience. Journal of Materials Science 39, 5887-5904, (2004).
- 2. F. MONTEVERDE, A. BELLOSI, L. SCATTEIA Processing and properties of ultra-high temperature ceramics for space applications. Mater. Sci. Eng. A 485, 415–421 (2008).
- 3. T. H. SQUIRE, J. MARSCHALL Material Property Requirements for Analysis and Design of UHTC Components in Hypersonic Applications. J. Eur. Ceram. Soc., 30 [11] 2239–51 (2010).
- 4. P. A, JAYASEELAN and al. UHTC composites for hypersonic applications. J. Am. Ceram. Soc., 91, 22–29 (2012)
- 5. W. G. FAHRENHOLTZ, E. J. WUCHINA, W.E. LEE, Y. ZHOU Ultra-High Temperature Ceramics: Materials for Extreme Environment Applications (2014).
- 6. J.F. JUSTIN Investigations of High Temperature Ceramics for Sharp Leading Edges or Air Intakes of Hypersonic Vehicles. 3<sup>rd</sup> EUCASS, Versailles, France, CD-ROM ISBN 978-2-930389-47-8, (2009).
- 7. J.F. JUSTIN and A. JANKOWIAK Ultra High Temperature Ceramics: Densification, Properties and Thermal Stability. AerospaceLab, issue 3 November 2011.
- M. BOUCHEZ and al. Combustor and Material Integration for high speed aircraft in the European research Program ATLLAS 2 (American Institute of Aeronautics and Astronautics, 2014). doi:10.2514/6.2014-2950
- 9. M. KUHN and al. Ceramic Strut Injection Technologies for High-Speed Flight. (American Institute of Aeronautics and Astronautics, 2017). doi:10.2514/6.2017-2416
- 10. J. STEELANT and al. Achievements obtained within ATLLAS II on Aero-Thermal Loaded Material Investigations for High-Speed Vehicles (21st AIAA International Space Planes and Hypersonics Technologies Conference, Xiamen, China, (AIAA 2017-2393), doi:10.2514/6.2017-2393

- 11. V. GUERINEAU Mécanismes et cinétiques d'oxydation de matériaux ultraréfractaires sous conditions extrêmes. Ph.D. Dissertation of Pierre et Marie Curie University (2017)
- 12. V. GUERINEAU, A. JULIAN-JANKOWIAK Oxidation mechanisms under water vapour conditions of ZrB<sub>2</sub>-SiC and HfB<sub>2</sub>-SiC based materials up to 2400°C. J. Eur. Ceram. Soc. 38, 421–432 (2018).
- 13. J.-F.JUSTIN, A. JULIAN-JANKOWIAK, V. GUERINEAU, V. MATHIVET, A. DEBARRE Ultra-high temperature ceramics developments for hypersonic applications. CEAS Aeronautical Journal 11 651-664 (2020)
- 14. V. GUERINEAU, G. VILMART, N. DORVAL, A. JULIAN-JANKOWIAK In situ study of the oxidation of ZrB<sub>2</sub> and ZrB<sub>2</sub>-SiC materials by monitoring the LIF signal of BO<sub>2</sub> radicals. Corrosion Science 148, 31-38 (2019)
- 15. V. GUERINEAU, G. VILMART, N. DORVAL, A. JULIAN-JANKOWIAK Comparison of ZrB<sub>2</sub>-SiC, HfB<sub>2</sub>-SiC and HfB<sub>2</sub>-SiC-Y<sub>2</sub>O<sub>3</sub> oxidation mechanisms in air using LIF of BO<sub>2</sub>(g). Corrosion Science 163
- 16. S-Q. GUO Densification of ZrB<sub>2</sub>-based composites and their mechanical and physical properties: a review. J Eur Ceram Soc; 29 (6):995-1011, (2009).
- 17. L. LI, Y. WANG, L. CHENG, L. ZHANG Preparation and properties of 2D C/SiC-ZrB2-TaC composites. Ceram. Int. 37, 891–896 (2011)
- 18. S. ZHANG, S. WANG, Y. ZHU, Z. CHEN Fabrication of ZrB<sub>2</sub>-ZrC-based composites by reactive melt infiltration at relative low temperature. Scripta Materialia. 65, 139-142 (2011).
- 19. A. PAUL, S. VENUGOPAL, J. BINNER and al. UHTC-Carbon fibre composites: Preparation, oxyacetylene torch testing and characterisation. J. Eur. Ceram. Soc. 33, 423-432 (2013)
- 20. L. SILVESTRONI, D.D. FABBRICHE, D. SCITI Tyranno SA3 fibre-ZrB2 composites. Part I: Microstructure and densification. Materials & Design, 65, 1253–1263 (2015)
- 21. M. KÜTEMEYER, L. SCHOMER, T. HELMREICH, S. ROSIWAL, D. KOCH Fabrication of ultra high temperature ceramic matrix composites using a reactive melt infiltration process. J. Eur. Ceram. Soc 36, 3647–3655 (2016)
- 22. S. TANG, C. HU Design, Preparation and Properties of Carbon Fibre Reinforced Ultra-High Temperature Ceramic Composites for Aerospace Applications: A Review. J. of Materials Science & Technology, 33, 117-130 (2017)
- 23. Q. LI, S. DONG, Z. WANG, G. SHI Fabrication and properties of 3-D C<sub>f</sub>/ZrB<sub>2</sub>-ZrC-SiC composites via polymer infiltration and pyrolysis. Ceramics International, 39, 5937-5941 (2013)
- 24. ASTM Standard E1876-09 Standard Test Method for Dynamic Young's Modulus, Shear Modulus, and Poisson's Ratio by Impulse Excitation of Vibration
- 25. G.R. ANSTIS and al A critical evaluation of indentation techniques for measuring fracture toughness: I. direct crack measurements, J. American Ceramic Society, 64, 534-553 (1981)
- 26. A. GÜLHAN, B. ESSER Arc-Heated Facilities as a Tool to Study Aerothermodynamic Problems of Reentry Vehicles. Progress in Astronautics and Aeronautics, Vol. 198, AIAA, 375-403 (2002)